Field Consolidation of Varved Clay
Report No. 4

by

Richard P. Long, Associate Professor
Kent A. Healy, Associate Professor

JHR 74-78 Project 70-3

This research was sponsored by the Joint Highway Research Advisory Council of the University of Connecticut and the Connecticut Department of Transportation, and was carried out in the Civil Engineering Department of the University of Connecticut.

ROUTE I-84 WEST HARTFORD

General

The data processed during this phase of the project on field consolidation of varved clay came from CONNDOT projects numbered 63-141, 63-151, 63-184 and 63-192 in West Hartford. These projects included both sand drained and non-sand drained areas. The primary purpose of using sand drains in some areas was to insure embankment stability by increasing the shear strength of the clay via rapid dissipation of hydrostatic excess pore pressure. The control of the post construction settlements was less important. The sand drains appear to have achieved the intended purpose. The pore pressures observed after each stage of filling were very small compared to the hydrostatic excess pore pressures that could have been generated by the amount of fill placed. As a result certain limitations must be placed on the interpretation and analysis of the data. The coefficients of consolidation extracted from the field data represent the minimum C_v values. The clay might be dissipating the pore pressures faster.

PROJECTS 63-151 AND 63-184

I. Consolidation Analysis

ICES-SEPOL program was again used to compute the distribution of stresses below the areas loaded by fills. Initial excess pore pressures were determined from the computed stresses by the equation:

$$u_o = \frac{\Delta\sigma_1 + \Delta\sigma_2 + \Delta\sigma_3}{3} \qquad (1)$$

The initial hydrostatic excess pore pressures predicted by Eq. 1 are probably slightly low. Equation 1 was used due to the lack of information on pore pressure parameters.

The initial excess pore pressure is again defined as the pore pressure that would be generated by the load were it placed instantaneously.

1. Sand Drained Areas

The piezometers in the sand drained area were assumed to be positioned midway between the sand wells. It was also assumed that the spacing of the sand wells equals the effective drainage diameter. The consolidation of the piezometer located at mid-depth of the clay layer was assumed to be influenced by consolidation in the horizontal direction only.

The initial filling sequences caused little or no hydrostatic excess pore pressure readings at the piezometers. This was taken as indicating rapid dissipation of excess pore pressures. Some of the final filling sequences resulted in small residual pore pressures that dissipated with time. The rapid dissipation of pore pressures allowed some evaluation of the coefficient of secondary compression.

a. Coefficient of Consolidation in the Horizontal Direction (C_h)

Values of C_h were determined from the rate of hydrostatic excess pore pressure dissipation at the mid-depth piezometer. In a region being serviced by sand drains, the greatest hydrostatic excess pore pressures occur along the midpoint between sand wells ($r = r_e$) at all times after dissipation has begun. The average percent consolidation for the clay layer is greater than the value at the radius r_e. It was decided to use Schiffman's Charts and Equations for Equal-Strain Sand-Drains

having constant permeability and linear loading (1). Schiffman's work is based on average values of consolidation so the consolidation at piezometer locations along the effective radius had to be converted to the average percent consolidation for the layer as a whole. To make these conversions, information from two figures (Fig. 7 and 8) from a paper by Johnson were used (2). The information from Johnson's paper is shown in Fig. 1 for a ratio of $n = \frac{r_e}{r_w} = 8$; where r_e = the effective radius of the sand drain and r_w = the radius of the sand well. Fig. 1(a) shows the variation of the point pore pressures $\frac{u}{u_o}$ at the effective radius of the drain as a function of the time factor T_h where $T_h = \frac{C_h t_h}{4 r_e^2}$. Fig. 1(b) shows the average consolidation for the region serviced by a sand drain as a function of T_h. Comparing values in both graphs at the same T_h shows that the average pore pressure in the region is lower than the pore pressures midway between the sand drains. From the graphs in Fig. 1, the ratio of the average pore pressures $\frac{\bar{u}}{\bar{u}_o}$ was determined for each piezometer reading of interest. The average ratio of pore pressures thus determined was used to find C_h from Schiffman's Equations. For cases at the end of construction, Eq. 27a was used (1). For the analysis reported here this equation reads:

$$\frac{\bar{u}}{\bar{u}_o} = \frac{1}{8T_o}\left[\overline{1.4}\right]\left[\overline{1 - e^{-8To/1.4}}\right] \qquad (2)$$

This equation was derived for the assumption of no smear and $n = 8$, where T_o = time factor at the end of construction, and is defined as $T_o = \frac{C_h t_o}{4 r_e^2}$. Computing $\frac{\bar{u}}{\bar{u}_o}$, in Eq. 2, from the

piezometer readings T_o can be solved for by trial and error. Then knowing the physical time of filling t_o, the coefficient of horizontal consolidation C_h can be computed.

Where no pore pressures were indicated at the end of filling an average consolidation of 90% $\left[\frac{\bar{u}}{\bar{u}_o} = 0.1\right]$ was assumed. When pore pressures persist after the filling is complete, the rate of dissipation of pore pressure can be used to determine the coefficient of horizontal consolidation at the middle piezometer in a similar fashion. Again the point consolidation at the middle piezometer must be used to determine the average pore pressure of the region $\left[\frac{\bar{u}}{\bar{u}_o}\right]$. Knowing $\frac{\bar{u}}{\bar{u}_o}$ and To, the time factor T_h for the spacing of the sand drains on this project can be determined from the equation: (2)

$$\frac{\bar{u}}{\bar{u}_o} = \frac{1}{8T_o}\left[\overline{}\right]\left[1 - e^{-8T_o/1.4}\right] e^{-8(T_h - T_o)/1.4} \qquad (3)$$

All the symbols are as defined before and T_h is defined as $T_h = \frac{C_h t_h}{4 r_e^2}$ where t_h is the physical time since filling began.

All the values of the C_h were determined either with Eq. 1 or Eq. 2. Fig. 2 shows the values of C_h found by these analyses as a function of the effective stress (insitu stress + stress due to filling) at the center piezometer when the analysis was made. As can be seen from Fig. 2, C_h decreases with increasing effective stress over the range of stresses analyzed. Also shown in Fig. 2 is the approximate value of the maximum past pressure in the vertical direction ($\bar{\sigma}_{Vm}$) determined from laboratory data. The effective

stresses acting on the soil appear to be approaching the maximum past pressure which is probably why C_h shows a strong decrease with increased effective stress.

The values of C_h resulting from this analysis have several shortcomings. The analysis had to work with low values of the hydrostatic excess pore pressure. More accurate values could be obtained if the consolidation process were observed over a larger change in pore pressures. The assumption of 90 percent consolidation when no pore pressures could be read may yield a value for C_h that is too small since a percent consolidation slightly greater than 90% represents a large change in the corresponding time factor and a correspondingly greater C_h. On the other hand, assuming that all of the dissipation of hydrostatic pore pressures in the mid-depth of the clay is due to consolidation in the horizontal direction results in values of C_h that are slightly large because some of the dissipation may take place in the vertical direction. Considering both of these errors, the values of C_h are probably slightly low.

b. Coefficient of Consolidation in the Vertical Direction C_v

It was assumed that the increased consolidation indicated by the piezometers between the mid-depth piezometers and the upper and lower edges of the clay layer was caused by dissipation of pore pressures in the vertical direction. It was further assumed that the contribution of horizontal dissipation of excess pore pressures was the same throughout the clay layer. The net percent consolidation was assumed to be the same as would have been

realized by considering the horizontal and vertical flow separately according to the equation: (3)

$$\left[\frac{u}{u_o}\right]_{h+v} = \left[\frac{u}{u_o}\right]_{v} \cdot \left[\frac{u}{u_o}\right]_{h} \qquad (4)$$

where $\left[\frac{u}{u_o}\right]_{h+v}$ = the observed hydrostatic excess pore pressure divided by the computed initial hydrostatic excess pore pressure; $\left[\frac{u}{u_o}\right]_{h}$ is the ratio of hydrostatic excess pore pressures computed from the rate of horizontal consolidation found at the center piezometer and; $\left[\frac{u}{u_o}\right]_{v}$ is the ratio of hydrostatic excess pore pressures due to vertical dissipation only.

From equation 4, $\left[\frac{u}{u_o}\right]_{v}$ can be computed at various times after filling began and the percent consolidation can be computed on a point basis from:

$$U_z = \left[1 - \left[\frac{u}{u_o}\right]_{v}\right] \times 100\% \qquad (5)$$

To determine C_{va}, the apparent coefficient of consolidation for time when the fill is at constant height Eq. 5 must be applied at successive times and the appropriate time factor found for each from an average consolidation curve (4). C_{va} is then found from:

$$\Delta T_v = \frac{C_{va}\,\Delta t}{H^2} \qquad (6)$$

In cases where C_{va} is desired for the filling, the physical construction time must be adjusted as $t_a = \frac{t_e}{2}$

where: t_a = adjusted time for computation and t_e = actual filling time.

The resulting C_{va}'s are shown in Figure 3 plotted against the vertical effective stress $\bar{\sigma}_v$. As can be seen, the general trend for these values is to decrease with increasing effective stress. There were, however, several exceptions which are probably due to all the assumptions and manipulation required to obtain the coefficient of vertical consolidation. The larger values of C_{va}'s for these projects seem to be slightly greater than those previously observed. The values previously computed required fewer assumptions and less manipulation.

At three piezometer locations the pore pressures at the center piezometer (B piez.) were always lower than the hydrostatic excess pore pressures indicated at the piezometers closer to the top and bottom of the clay layer. The change in pore pressure readings in the center piezometer showed regular dissipation. One explanation of the observed behavior is that these three locations contain a thin permeable layer near mid-depth. The data were analyzed using this assumption; the results are shown in Table I. The term upper layer denotes the varved clay between the assumed internal sand seam and the maximum elevation of varved clay at that point. The term lower layer denotes the varved clay between the assumed internal sand seam and the minimum elevation of the varved clay. As can be seen from Table I analysis using this assumption yields reasonable values for the coefficients of consolidation which are approximately the same for the upper and lower layers. Analysis was also conducted assuming that the entire layer was homogeneous and ignoring the piezometer readings at the center of the layer and working only

TABLE I

Apparent Coef. of Consolidation in the Vertical Direction
Values in Areas Which May Contain a Sand Seam

	Layer	I84-5	WE-1 (During Filling)	WE-2	I84-5 (After Filling)
C_h	upper	3.4	1.3	1.2	2.9
ft^2/day	lower	6.7	1.4	0.9	3.8
C_v	upper	2.2	0.3	0.3	0.7
ft^2/day	lower	2.0	0.1	0.1	0.9

TABLE II

Result of the Non-sand Drained Area Analysis - Computation of the C_v is based on considering total thickness of clay as one layer

Piez. No.	Height of fill (ft)	Thickness of Clay (ft)	C_v ft^2/day
EW-1	26	92	2.8
EW-2	11	92	5.9
EW-3	11.5	75	3.3
EW-4	13.5	72	2.8

with the piezometers near the upper and lower boundaries. This approach yielded C_{va} values much lower than the method assuming the internal sand seam. If the analysis had yielded coefficient of consolidation values that are too high this would tend to make the consolidation settlement values (ρ_c) too small and the coefficient of secondary compression values (C_α) too big. However, the values of each of these parameters evaluated by this technique were on the low side of the range of values for all locations.

2. Non-sand Drained Areas

The non-sand drained areas were analyzed as reported previously (4)(5)(6). The results are shown in Table II.

II. Secondary Compression

The sand drains allowed rapid dissipation of hydrostatic excess pore pressures in this region. Settlement observations continued for long enough times to make an estimate of the coefficient of secondary compression (C_α) which was taken as:

$$C_\alpha = \frac{\Delta H_{sc}/H}{\log t_{2/t_1}} \tag{7}$$

where: ΔH_{sc} = amount of settlement after excess pore pressures are complete; H = thickness of the clay layer; t_1 = estimated time of 100% consolidation; t_2 = time after t_1 when the secondary compression settlement equals ΔH_{sc}.

At some of the piezometer locations a decrease in the elevation of the water table during the summer months could be observed. The settlement due to lowering of the ground water table was estimated by the equation:

$$\rho_a = \Delta\bar{\sigma}_v \cdot M_v \cdot H \tag{8}$$

where: $\Delta\bar{\sigma}_v$ = change in effective stress due to ground water lowering, taken here = $\Delta h \cdot \gamma_w$; Δh = change in ground water elevation in feet; γ_w = unit weight of water; M_v = coefficient of volume compressibility, taken = 0.85% $\frac{ft^2}{ton}$ (from previous reports).

The secondary compression was taken as the observed settlement between t_1 and t_2 minus the correction for water table lowering. The values of C_α resulting from this analysis are shown in Figure 4 plotted against the log of the effective vertical stress at mid-depth of the clay layer. The values of C_α plotted in Figure 4 are scattered. Although a curve can be drawn, the plot indicates no general trend. The effective stresses at the mid-depth of the clay layer are close to the effective precompression stress. The clay in the upper portion of the layer may well be in the normally consolidated region while the clay in the lower part of the layer at the same point may still be overconsolidated.

III. Initial Settlements

The field data from the sand drained areas were difficult to analyze for initial settlements. The small hydrostatic excess pore pressures, remaining after most fill increments were completed, made the evaluation of the percent average consolidation hard to determine with any accuracy. In many cases a percent consolidation was assumed in the evaluation of a coefficient of consolidation. This assumed percent consolidation did not work as well for the initial settlements.

An extensive analysis of the square root of adjusted time plots for sand drained areas was made. The following conclusions were drawn from the analysis:

1. The percent consolidation after filling was too high . The observed settlement data plotted against the square root of adjusted time under these conditions will not form a straight line that can be extrapolated to eliminate the consolidation settlements.
2. The plots of theoretical solutions of the square root of the time factor against the average percent consolidation do not extrapolate through the origin, unless the coefficient of consolidation decreases by a factor of 10 during the consolidation process. See Fig. 5. The data for Fig. 5 were taken from Schiffman (1). The parameter C_o represents the coefficient of consolidation at the beginning of consolidation and C_f, the coefficient of consolidation at the end.

Initial settlements were not, therefore, extracted from the data for settlement platforms in the sand drained areas.

The square root of adjusted time method allowed initial settlements to be extracted from the settlement data for the non-sand drained areas. The results are shown in Table III and plotted in Fig. 6.

IV. Total Settlements

1. Sand Drained Areas

In the sand drained areas only the total settlements could be extracted since it was not possible to separate the initial from the consolidation settlements. These values are shown in Fig. 7. The plot in Fig. 7 shows that the use of the value of M_v = 0.85% ft^2/ton without also accounting for initial settlement underestimates the

TABLE III

Initial Settlement for Project 63-184 (Non-Sand Drain Area)

PL No.	Ht. of Fill (ft)	Width of Fill (ft)	Dist. from Center of Fill (ft)	Initial Settlement (ρ_i)
1	18.5	96	26	+0.33
1A	18.5	96	34	+0.28
11	13	64	12	+0.26
12	13	60	14	+0.26
14	26	108	25	+0.05
21	11	92	6	+0.1

settlements experienced in the field. Use of the average laboratory value of M_v = 2.5% ft^2/ton overestimates most settlements observed in the field. These settlements were computed with ICES-SEPOL.

2. Non-Sand Drained Areas

In these areas the initial and consolidation settlements could be separated. The plot of initial settlements is shown in Fig. 6. The plot of consolidation settlements is shown in Fig. 8.

PROJECTS 63-141 AND 63-192

I. Consolidation Analysis

The piezometer response on these projects tended to be irregular. On Project 63-141 (sand drained area) only the data from piezometer groups 5, 6, 7 and 15 could be analyzed. Each of these areas was sand drained. The assumptions used in the analysis were the same as those used on Projects 63-151 and 63-184. The coefficients of consolidation are shown in Table IV.

Piezometer Group 5 had only one piezometer so it was not possible to analyze the data for the vertical coefficient of consolidation. The "C" piezometer at Groups 6, 7 and 15 showed no dissipation which may be due to malfunction. The values shown for the coefficient of vertical consolidation were determined from the readings at the "A" piezometer only.

TABLE IV

	During Construction		After Construction	
Piez No.	C_h (ft^2/day)	C_v (ft^2/day)	C_h (ft^2/day)	C_v (ft^2/day)
5	1.57	- -	0.172	- -
6	1.57	(Pt A) 8.0 (Pt C) -	2.2	(Pt A) 3.45 (Pt.C) - -
7	0.96	(Pt A) 5.6 (Pt C) 12	0.35	(Pt A) 2.56 (Pt C) - -
15	6.5	(Pt C) 2.44	1.3	(Pt C) --

The method of D'Appolonia et al (7) was developed for strip loading so the fill cross-sections were approximated by equivalent strips. The overconsolidation ratio was then determined at a depth under the center of the loaded area equal to B/2, where B equals the width of the equivalent strip. The overconsolidation ratio is defined as $OCR = \frac{\bar{\sigma}_m}{\bar{\sigma}_v}$, where $\bar{\sigma}_m$ equals the maximum past pressure indicated by one-dimensional laboratory consolidation tests and $\bar{\sigma}_v$ equals the vertical effective stress at a depth of B/2 due to the weight of the overburden. The overconsolidation ratio at this depth is important because stress analysis indicates that it is the first point which will experience plastic strains. Using this overconsolidation ratio an initial shear stress ratio "f" is determined from Fig. 9b.

The amount of plastic strain is related to the factor of safety with respect to bearing capacity. The factor of safety was computed by comparing the surface load due to the fill ($\gamma_t \cdot h$) with the ultimate bearing capacity ($q_u = 5.2\ S_u$) in the equation:

$$\frac{q}{q_u} = \frac{h \cdot \gamma_t}{5.2\ S_u} \qquad (9)$$

where: h = height of fill, γ_t = the approximate total unit weight of the fill material; q = the bearing pressure produced by the fill; S_u = the undrained strength of the clay and q_u = bearing capacity of the clay.

The values of the ratio q/q_u and f are used in Fig. 9a to determine the initial settlement ratio $S_R = \rho_e/\rho_i$. The initial settlement ratio relates the settlement due to elastic shear strain,

ρ_e, to the magnitude of the combined initial settlement ρ_i.

The values for initial settlements were computed in several steps. The amount of initial settlement due to elastic strains (ρ_e) was computed using ICES-SEPOL and the assumed undrained Young's Modulus. With the appropriate value of the overconsolidation ratio the value of f was selected from Fig. 10b. Knowing q/q_u and f the initial settlement ratio (S_R) was selected from the proper graph in Fig. 9a and the computed value of ρ_e used to determine ρ_i. The consolidation settlements were also computed with ICES-SEPOL. The sum of the computed initial settlement and consolidation settlement at each platform was taken as the total settlement.

The computed total settlements were compared with the settlements observed in the field 84 days after the end of filling. The results are shown in Table V. As can be seen the total settlements observed in the field tend to be slightly higher than the calculated settlements. The largest discrepancies are at settlement platforms 5 and 21. The observed settlements at platform 21 as well as platforms 19 and 20 which were in the same vicinity indicated a larger initial settlement than the other platforms reported in Table V. This might be due to the varved clay in this area being softer than the other areas or this area may have become somewhat disturbed when the sand drains were placed.

The average volume compressibility (M_v) for most of these platforms was also computed. These computations were based on

TABLE V

PL. No.	Ht. of fill (ft)	Width of fill (ft)	Thk of Clay (ft)	ρ_t - from ICES-SEPOL (ft)	ρ_t - est from field data (ft)	Max. Observed Settlement (ft)
5	5	88	72	0.17	0.37	0.46
8	13	136	76	0.65	0.7	0.73
15	14	104	68	0.58	0.65	0.65
16	16	86	60	0.58	0.85	0.96
21	14	88	56	0.47	1.2	1.3
22	10	88	88	0.48	0.62	0.75
23	10	88	88	0.48	0.48	0.62

the total settlement and the equation used was:

$$M_v = \frac{\rho_t}{\Delta\sigma_v \cdot h} \qquad (10)$$

where: $\Delta\sigma_v$ is the stress increment at mid-depth of the clay caused by the fill and h is the thickness of the varved clay. The results are shown in Table VI. The values of M_v reported in Table VI are higher than those determined from the previous projects but compare with the values extracted from laboratory tests and listed in the Appendix.

TABLE VI

PL No.	Ht. of fill (ft)	M_v (ft^2/T)
5	5	0.03
8	13	0.0131
16	16	0.0204
21	14	0.0374
22	10	0.0166

APPENDIX

Laboratory Compression Results

Determined from Laboratory Test Data for Volume Compressibility
(Project 63-184)

Boring No.	Depth	M_v (ft^2/T) recompression	M_v (ft^2/T) virgin compression	M_v (ft^2/T) reload cycle	C_c
B13-6(U)	10'-12'	0.028 (0.5-1)*	0.032 (3-4)*	- - - -	0.556
	10'-12'	0.03 (0.5-1)	0.032 (3-4)	0.0061 (0.5-1.5)*	0.662
	15'-17'	0.04 (0.5-1)	0.014 (3-4)	- - - -	0.365
	15'-17'	0.026 (0.5-1)	0.023 (3-4)	0.00655 (0.75-2)	0.365
	25'-27'	0.032 (0.5-1)	0.0357 (3-4)	0.0043 (1-2)	0.59
	40'-42'	0.024 (0.5-1)	0.022 (3-4)	- - - -	0.543
	40'-42'	0.026 (0.5-1)	0.013 (3-4)	0.0096 (1.3-2.8)	0.385
B14-7(U)	10'-11'	0.019 (0.5-1)	0.0102 (3-4)	- - - -	0.24
	10'-11'	0.015 (0.5-1)	0.009 (3-4)	0.004 (0.5-1.5)	0.243
	20'-22'	0.024 (0.5-1)	0.0308 (3-4)	0.0067 (1-2)	0.54
	20'-22'	0.03 (0.5-1)	0.034 (3-4)	- - - -	0.593
	25'-27'	0.04 (0.5-1)	0.014 (3-4)	- - - -	0.28
	25'-27'	0.04 (0.5-1)	0.032 (3-4)	0.0062 (1-2)	0.577
	30'-32'	0.017 (0.5-1)	0.013 (3-4)	- - - -	0.31
	30'-32'	0.0248 (0.5-1)	0.023 (3-4)	0.0052 (1.2-2.5)	0.5
	40'-42'	0.0254 (0.5-1)	0.014 (3-4)	- - - -	0.367
	40'-42'	0.026 (0.5-1)	0.022 (3-4)	0.0042 (1.4-2.7)	0.398
	45'-47'	0.043 (0.5-1)	0.032 (3-4)	- - - -	0.625
	45'-47'	0.031 (0.5-1)	0.0092 (3-4)	0.0035 (1.5-2.8)	0.24
B10-16(U)	65'-67'	0.024 (0.5-1)	0.0101 (3-4)	0.01 (1.8-3)	0.276
	65'-67'	0.026 (0.5-1)	0.018 (3-4)	- - - -	0.564
B10-2(U)	15'-17'	0.018 (0.5-1)	0.035 (3-4)	- - - -	0.79
	35'-37'	0.035 (0.5-1)	0.033 (3-4)	- - - -	0.663
	35'-37'	0.049 (0.5-1)	0.022 (3-4)	0.0043 (1.5-3.5)	0.43

*numbers in parenthesis represents load range in Tons/ft^2

Determined from Laboratory Test Data for Volume Compressibility
(Project 63-141)
(From Lab Test Data)

Boring No.	Depth	M_v (ft^2/T) recompression	M_v (ft^2/T) virgin compression	M_v (ft^2/T) reload cycle	C_c
7	8'-10'	0.00295 (1.6-3.2)*	0.0119 (3.2-6.4)*	0.003 (1.5-3.2)*	0.354
	12.7'-14.7'	0.0189 (0.5-1)	0.0724 (2-4)	0.04 (1-2)	1.33
21	32'-34'	0.0222 (0.6-1.3)	0.035 (2.5-5)	0.0086 (1-2)	0.63
	94'-96'	0.012 (1.2-2.4)	0.026 (5-10)	0.0088 (2.5-5)	0.795
33	12'-14'	0.0152 (0.5-1)	0.046 (2-4)	0.015 (0.5-1.0)	0.77
	65'-67'	0.0236 (1-2)	0.0386 (4-7)	- - - - - - - - -	1.2
68	45'-47'	0.0229 (0.5-1)	0.04 (2-4)	- - - - - - - - -	0.57
	100'-102'	0.0098 (1-3)	0.0042 (10-20)	- - - - - - - - -	0.35
75	30'-32'	0.0288 (0.8-1.6)	0.019 (3.2-6.4)	0.01 (1.6-3.2)	0.53
	37'-39'	0.0148 (0.8-1.8)	0.0486 (1.8-3.5)	0.011 (1-2)	0.6
	45'-47'	0.0156 (0.45-1.8)	0.0123 (3.6-7)	- - - - - - - - -	0.28
	52'-54'	0.0284 (0.53-1.05)	0.0138 (2.1-4.3)	- - - - - - - - -	0.32
	52'-54'	0.0175 (1-2)	0.05 (2.2-4.2)	0.015 (1-2)	0.7
	60'-62'	0.0224 (0.8-1.5)	0.0154 (3.2-6.4)	0.006 (1.5-3)	0.35

$$M_v = \frac{\frac{\Delta e}{1 + e_o}}{\Delta \bar{\sigma}_v} \quad ; \quad C_c = \frac{\Delta e}{\Delta \log \bar{\sigma}_v}$$

*number in parenthesis represents load range in Tons/ft^2

REFERENCES

1. Schiffman, R.L., "Field Applications of Soil Consolidation Under Time-Dependent Loading and Varying Permeability", NAS-NRC, Highway Research Board Bull. 248, 1960.

2. Johnson, S.J., "Foundation Precompression with Vertical Sand Drains", Proc. ASCE, Jour. of Soil Mechanics and Foundation Division Vol. 96, SM1, Jan. 1970, pp. 145-175.

3. Scott, R.F., "Principles of Soil Mechanics", Addison-Wesley, 1963, pp. 204.

4. Long, R.P. and Healy, K.A., Preliminary Report, "Field Consolidation of Varved Clay, Phase I", Dept. of Civil Engr., U.Conn., JHRAC Project 70-3, JHR-PR 71-34, Jan. 1971.

5. Long, R.P. and Healy, K.A., "Field Consolidation of Varved Clay Report No. 2", Dept. of Civil Engr. JHRAC Project 70-3, JHR 71-38, June 1971.

6. Long, R.P. and Healy, K.A., "Field Consolidation of Varved Clay Report No. 3", Dept. of Civil Engr. JHRAC Project 70-3, JHR 72-55, Aug. 1972.

7. D'Appolonia, D.J., Poulos, H.G. and Ladd, C.C., "Initial Settlement of Structures on Clay", Proc. ASCE, Jour. of Soil Mechanics and Foundations Division, Vol. 97, No. SM10, Oct. 1971, pp. 1359-1377.

LEGEND FOR DIAGRAMS

Figure 1 — Comparison of the point consolidation at $r = r_e$ and the average consolidation for a sand drained area.

Figure 2 — Plot of the coefficient of horizontal consolidation (C_h) against vertical effective stress ($\bar{\sigma}_v$)

Figure 3 — Plot of the coefficient of vertical consolidation (C_v) against vertical effective stress ($\bar{\sigma}_v$)

Figure 4 — Plot of the coefficient of secondary compression against vertical effective stress ($\bar{\sigma}_v$)

Figure 5 — Theoretical Square Root of Time Factor plots for sand drained areas showing a decrease in the coefficient of consolidation during dissipation of pore pressures

Figure 6 — Plot of initial settlements for the non-sand drained areas

Figure 7 — Plot of total settlements for sand drained areas

Figure 8 — Plot of consolidation settlements for non-sand drained areas

Figure 9 — Diagrams used in the prediction of initial settlements

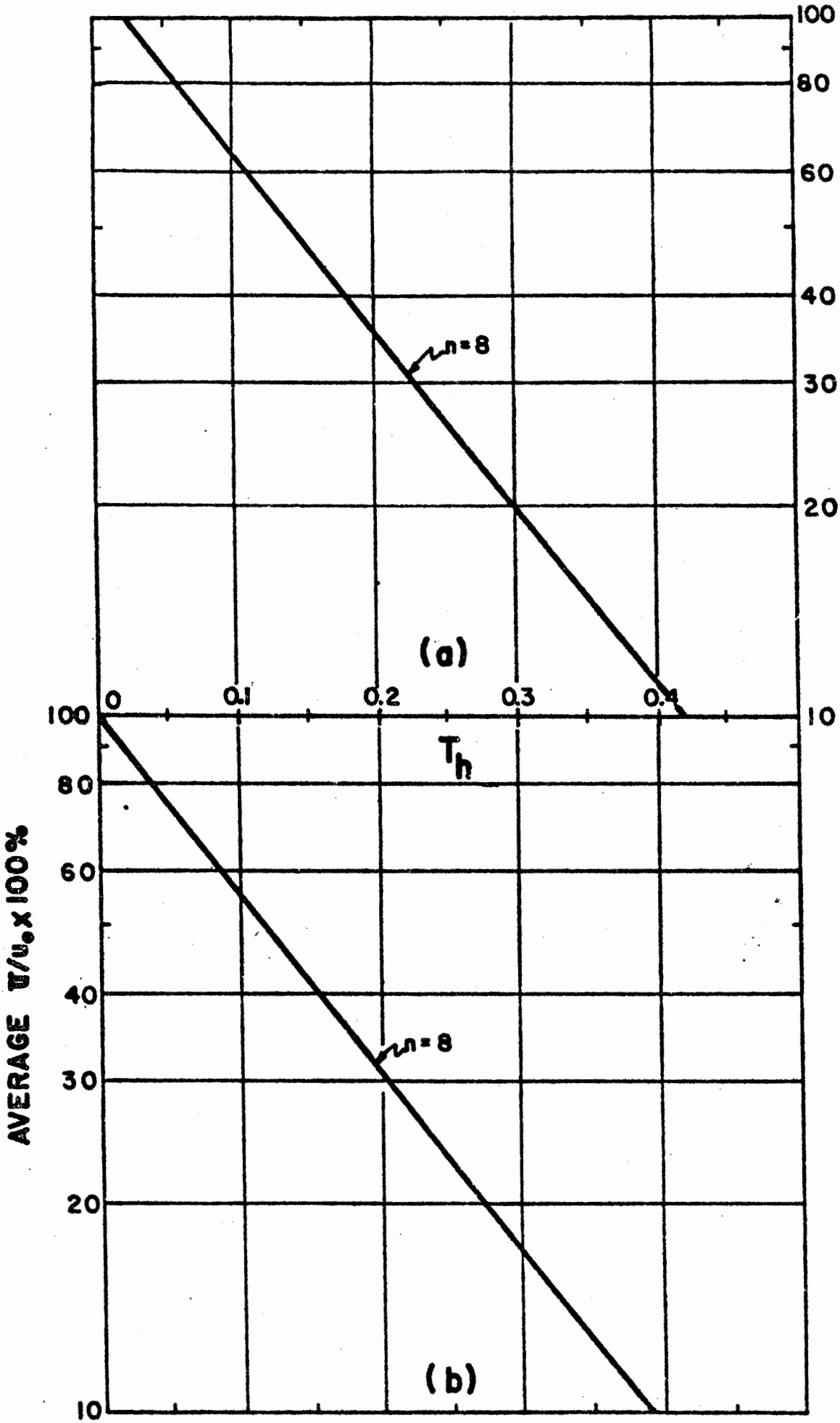
100
80
60
40
30
20
10
n=8
(a)
0
0.1
0.2
0.3
0.4
T_h
$u/u_o \times 100\%$ at $r = r_o$
AVERAGE $U/u_o \times 100\%$
n=8
(b)

FIGURE 1

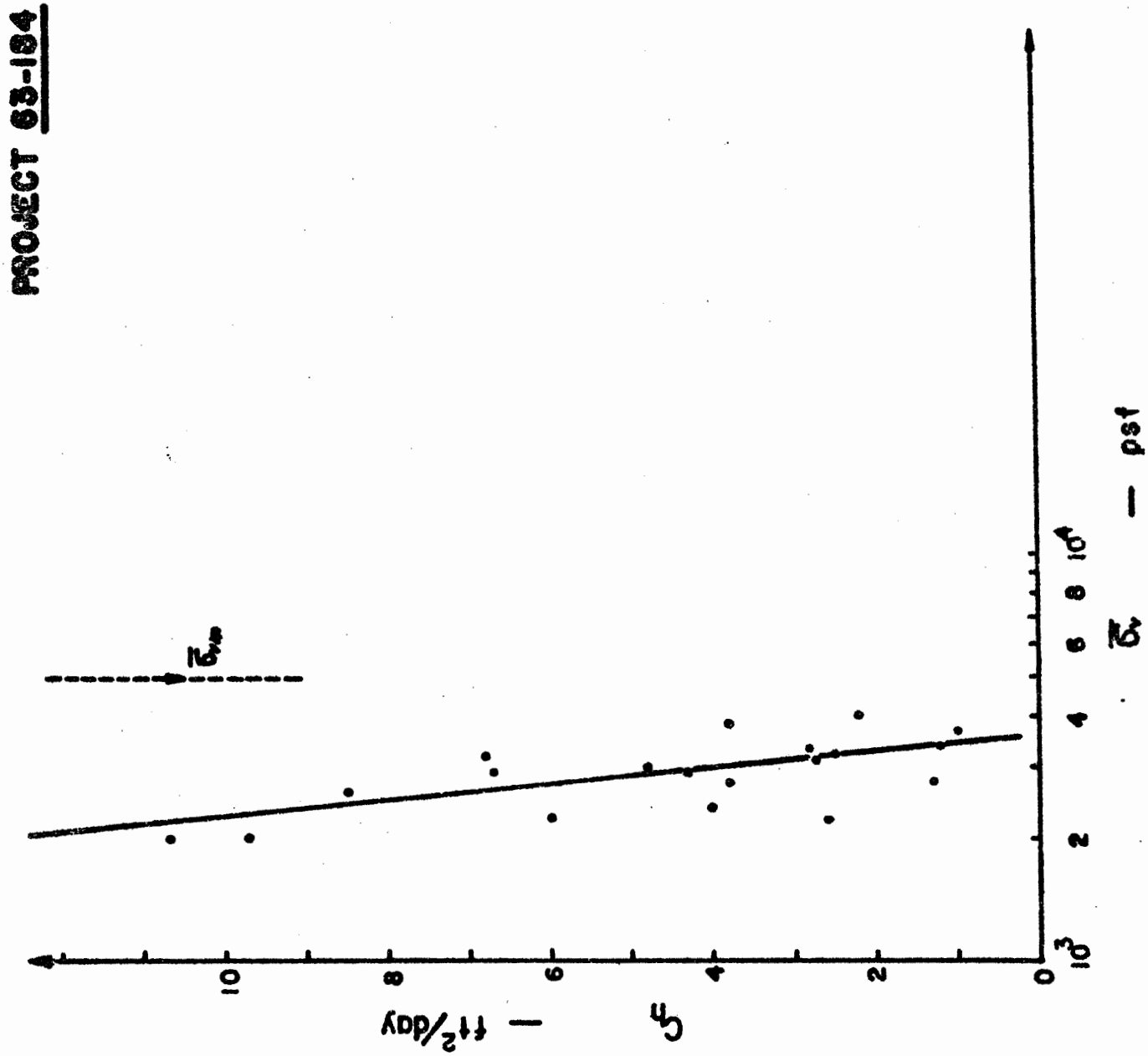
PROJECT 63-184
σ_{max}
σ_r — psi
10^3
2
4
6
8
10^4
0
2
4
6
8
10
σ_ξ — Ω^2/dqy

FIGURE 2

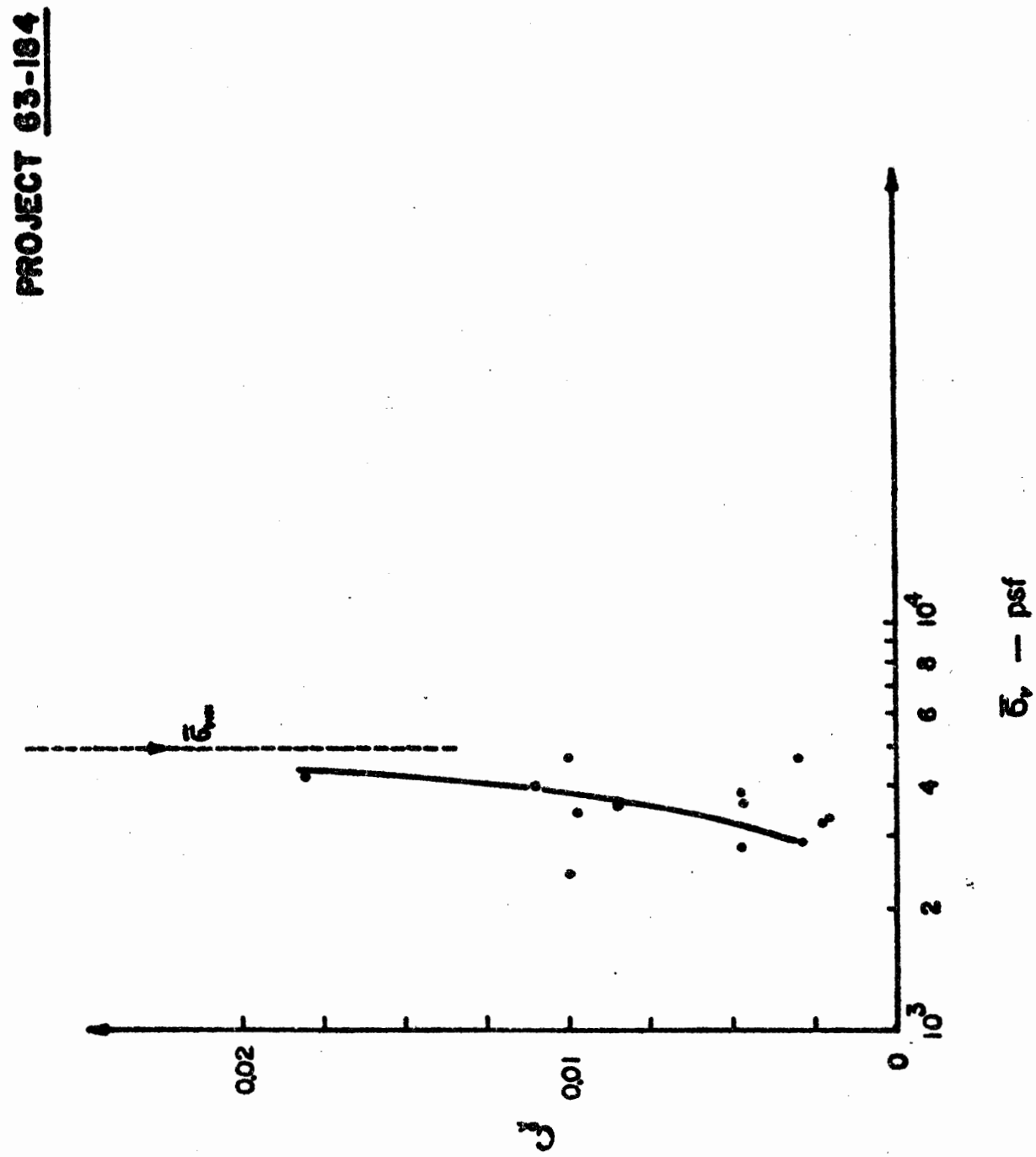
PROJECT 63-184
ε_{max}
0.02
0.01
0
10^3
2
4
6
8
10^4
$\bar{\sigma}_v$ — psf

FIGURE 4

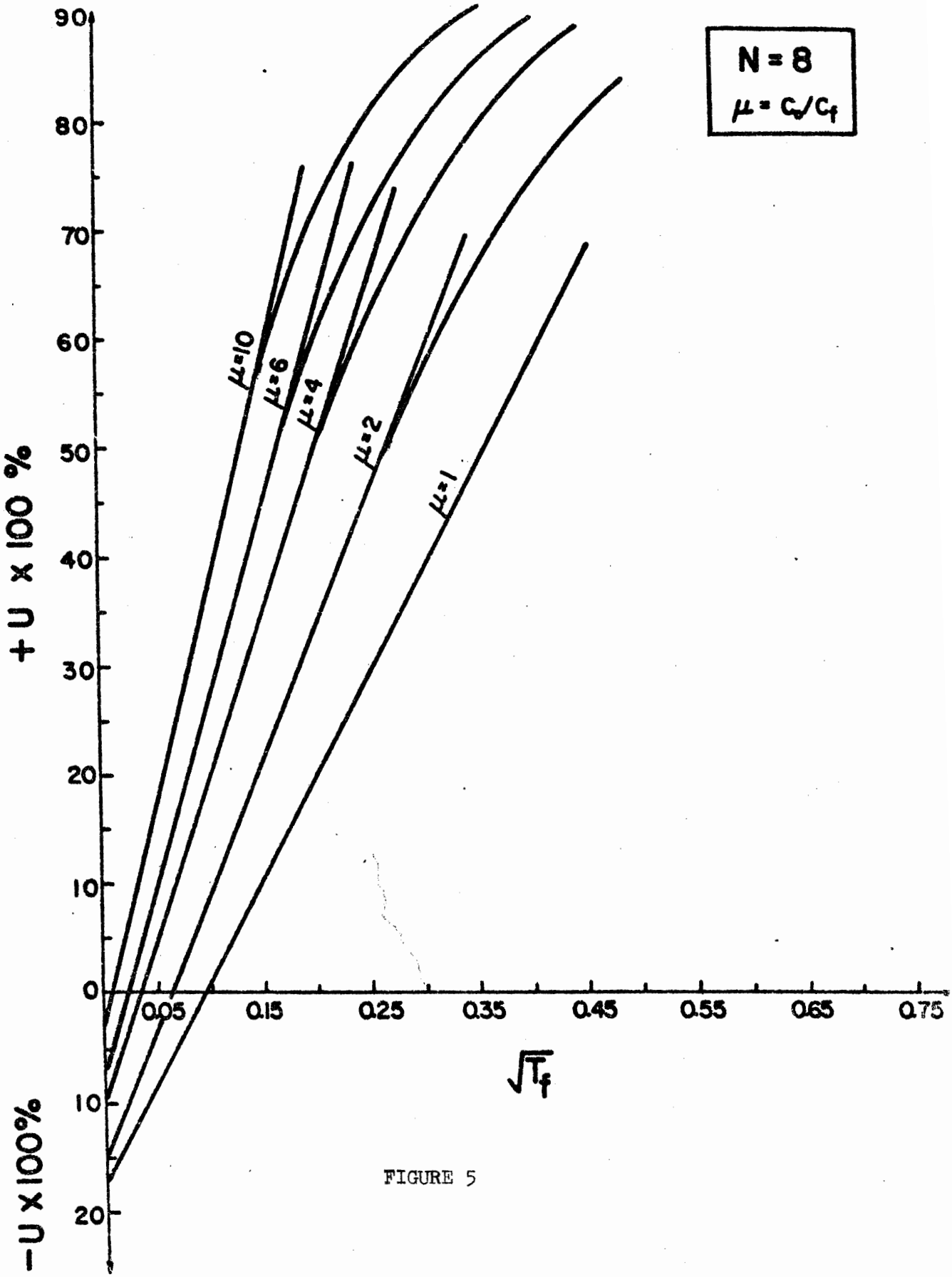
N = 8
μ = C/Cf
μ=10
μ=6
μ=4
μ=2
μ=1
+U x 100 %
-U x 100%
90
80
70
60
50
40
30
20
10
0
10
20
0.05
0.15
0.25
0.35
0.45
0.55
0.65
0.75
√Tf

FIGURE 5

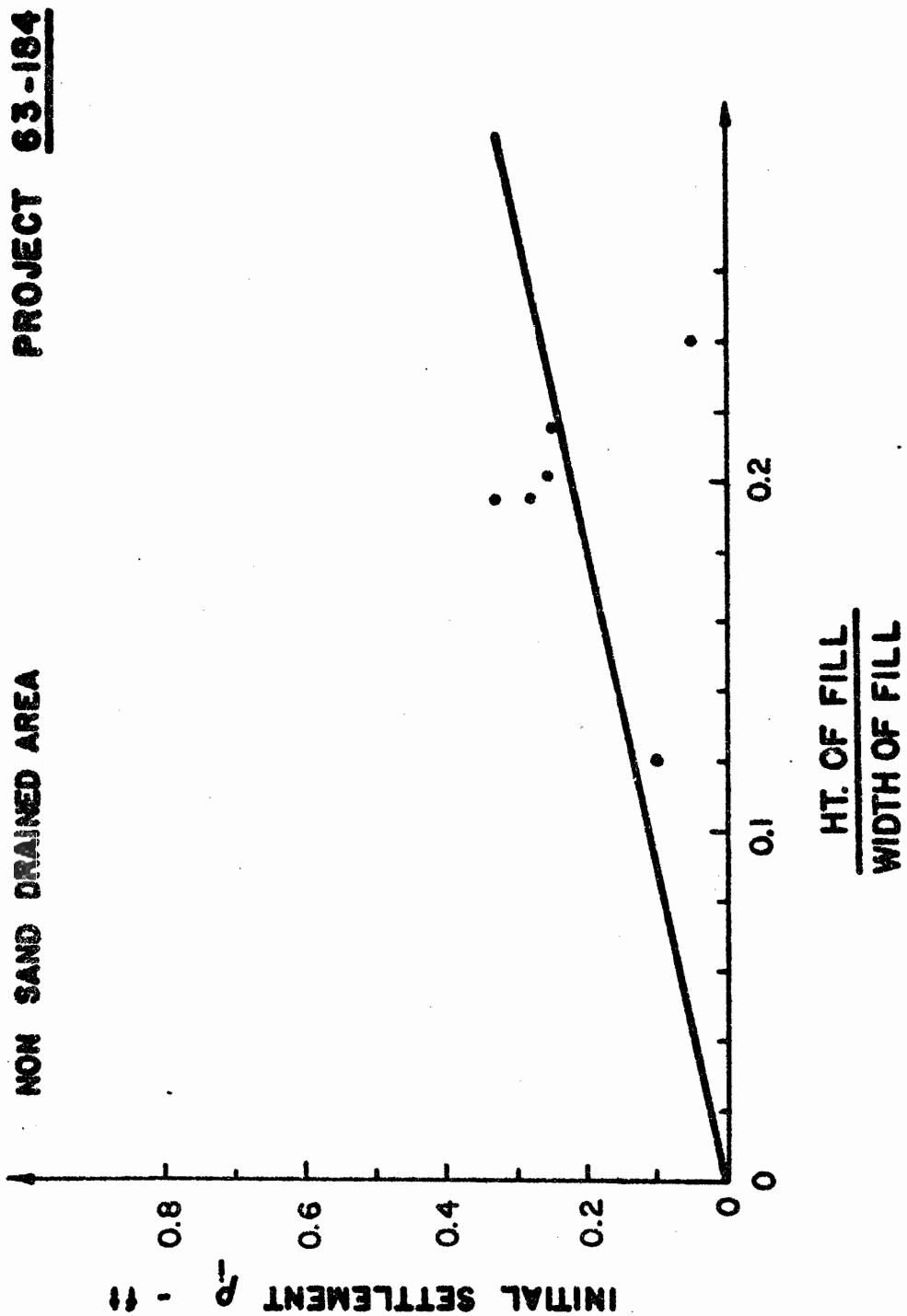
PROJECT 63-184
NON SAND DRAINED AREA
INITIAL SETTLEMENT ρ - ft
0.8
0.6
0.4
0.2
0
0.1
0.2
HT. OF FILL
WIDTH OF FILL

FIGURE 6

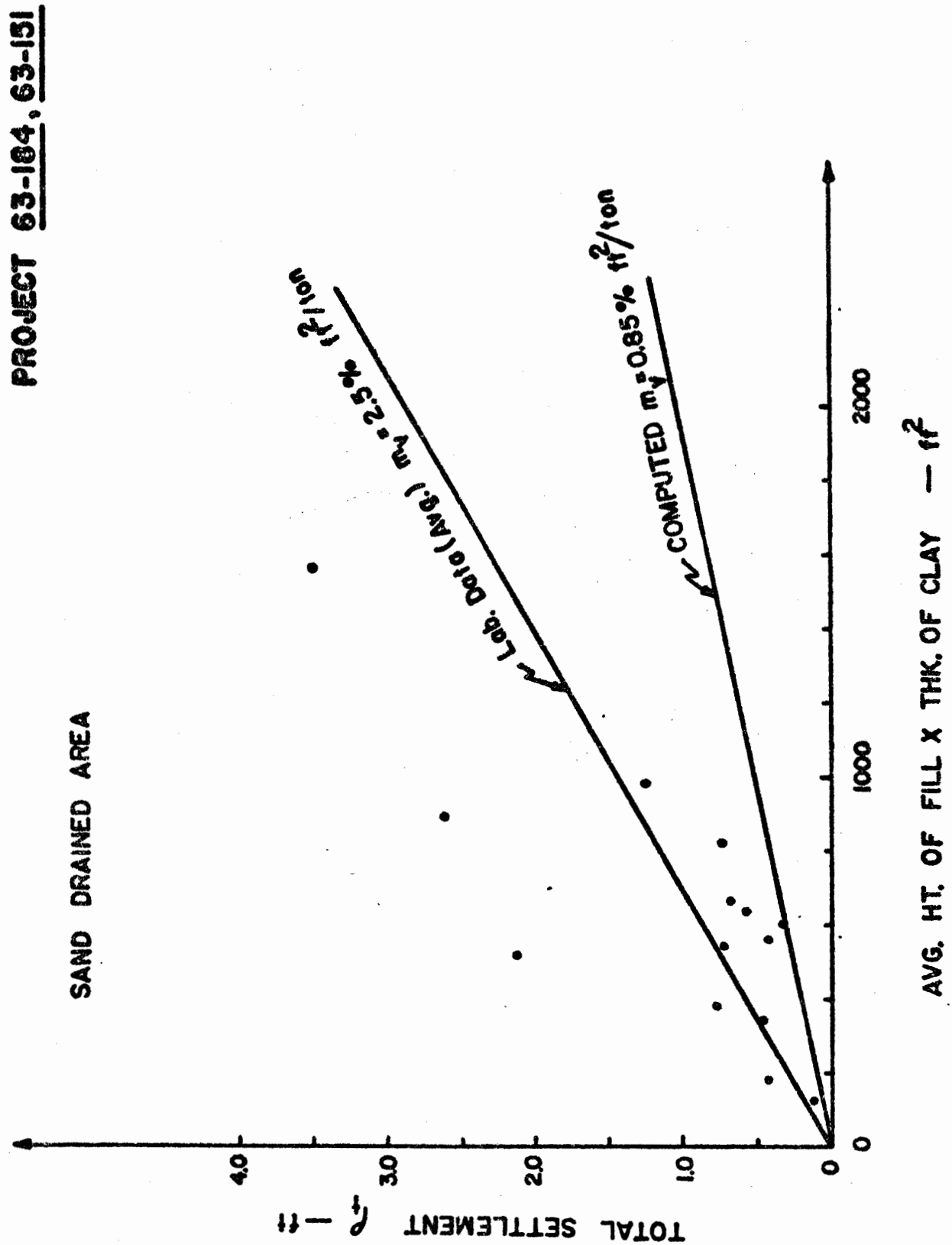
PROJECT 63-184, 63-151
SAND DRAINED AREA
Lab. Data (Avg.) m_v = 2.5% ft²/ton
COMPUTED m_v = 0.85% ft²/ton
TOTAL SETTLEMENT ρ — ft
AVG. HT. OF FILL X THK. OF CLAY — ft²
0
1.0
2.0
3.0
4.0
1000
2000

FIGURE 7

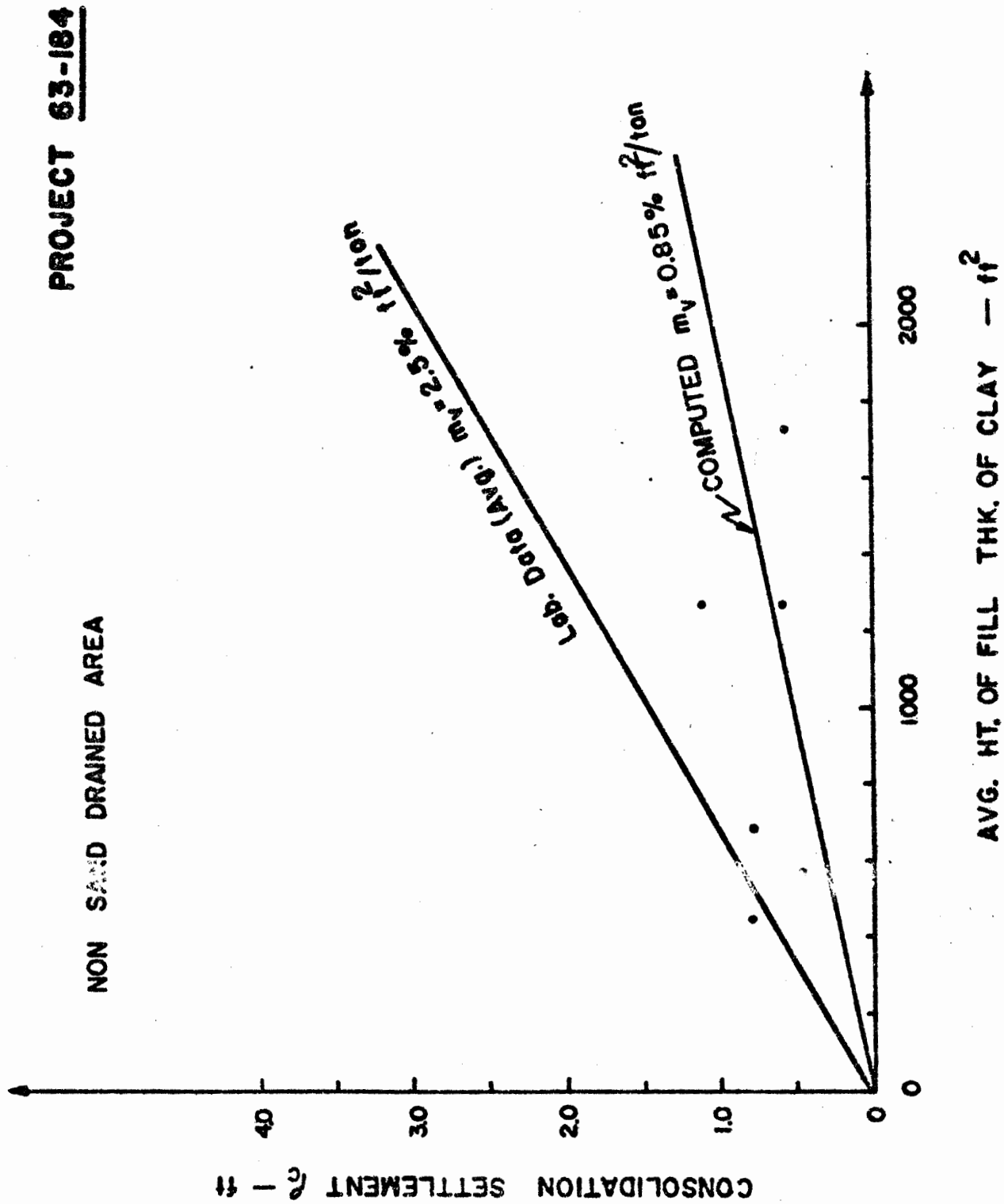
PROJECT 63-184
NON SAND DRAINED AREA
Lab. Data (Avg.) m_v=2.5% ft²/ton
COMPUTED m_v=0.85% ft²/ton
CONSOLIDATION SETTLEMENT S — ft
0
1.0
2.0
3.0
4.0
0
1000
2000
AVG. HT. OF FILL THK. OF CLAY — ft²

FIGURE 8

c.f. D'Appolonia et al

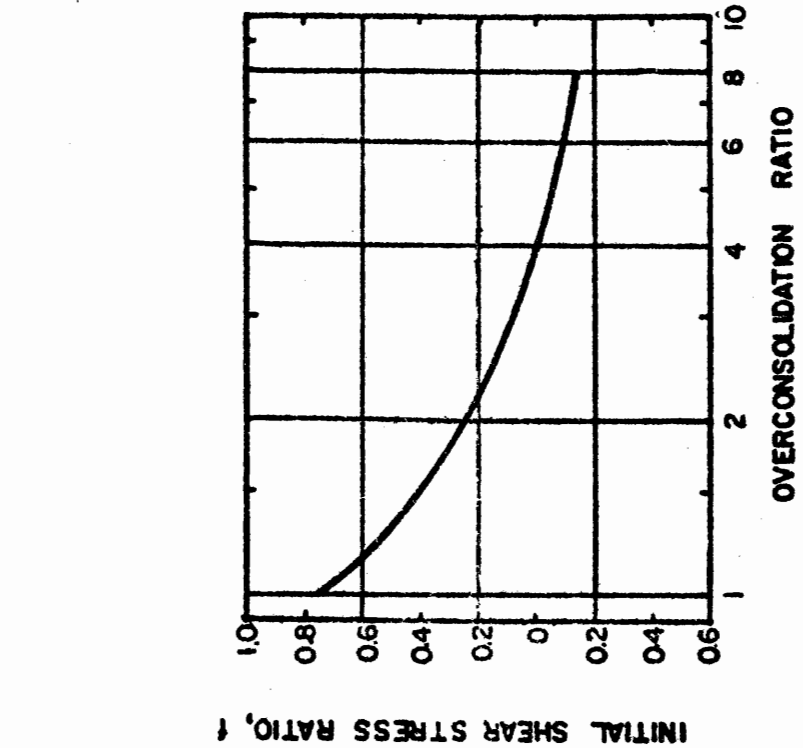

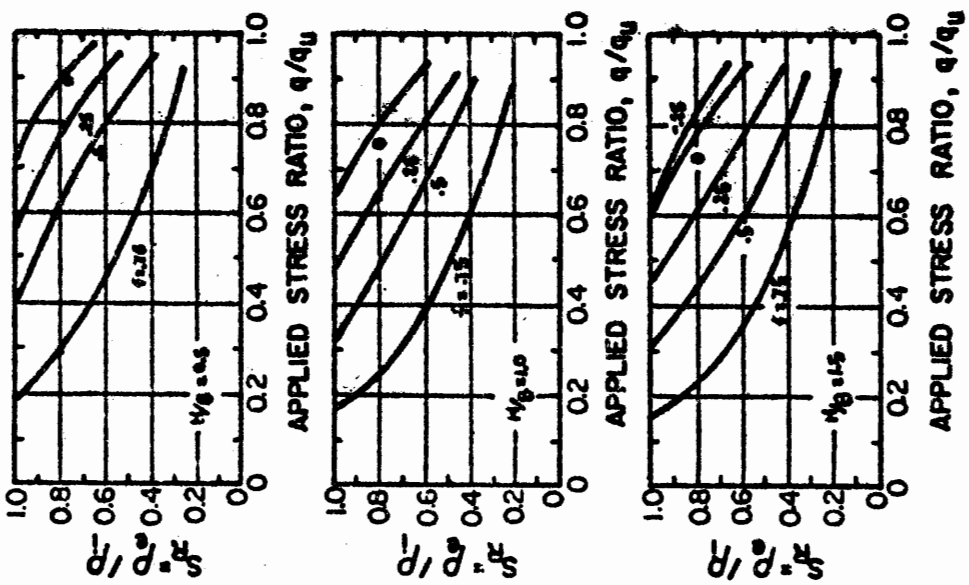

FIGURE 9